

## THE IRRESISTIBLE CHARM OF A SIMPLE CURRENT FLOW PATTERN – 25% WITH A SOLAR CELL FEATURING A FULL-AREA BACK CONTACT

S. W. Glunz, F. Feldmann, A. Richter, M. Bivour, C. Reichel, H. Steinkemper, J. Benick, M. Hermle

Fraunhofer Institute for Solar Energy Systems, Heidenhofstr. 2, D-79110 Freiburg, Germany  
Phone +49-761-4588-5191; Fax +49-761-4588-9250, email: stefan.glunz@ise.fraunhofer.de

**ABSTRACT:** Screen-printed Al-BSF silicon solar cells have dominated the PV market for decades. Their long-term success is based on a low-complexity cell architecture and a robust production sequence. The full-area rear contact allows a simple and effective one-dimensional current flow pattern in the base resulting in high fill factors. Some of the successor technologies of this simple but yet successful cell architecture, i.e. partial rear contact (PRC) and interdigitated back contact (IBC) solar cells, have a significantly higher process and pattern complexity. This paper discusses a cell structure with an architecture very similar to the classical screen-printed aluminium back surface field (Al-BSF) solar cell but with a higher efficiency potential. This is achieved by substituting the full-area doped back surface region by a passivated contact scheme consisting of a tunnel oxide covered by a heavily doped silicon film, called TOPCon. The champion efficiency of 25.1% on *n*-type silicon shows that this structure has a high potential while keeping the process effort low and the current flow pattern simple. The very high open circuit voltage of 718 mV and fill factor of 83.2% results from both, the very low recombination and transport losses caused by this contact scheme and cell architecture.

**Keywords:** Silicon, High-efficiency, Contact

### 1. INTRODUCTION

Interdigitated back contact (IBC) silicon solar cells are obviously an excellent choice to achieve world record efficiencies as has been proven by several groups [1-3]. Until 2014 the efficiency record was held by a cell structure with partial rear contact (PRC), i.e. the Passivated Emitter Rear Locally-diffused (PERL) cell structure [4, 5]. Both cell structures have in common that they are based on a strongly two or three dimensional contact pattern, either the interdigitated back grid of IBC cells or the local rear contact points of PRC cells. In fact, this lateral pattern has a much larger dimension than the thickness of the silicon wafer. Typical IBC cells have a contact pitch in the range of one mm while the thickness of the cell is around 0.15 mm which is nearly one order of magnitude smaller. In industrial PRC cells this ratio is not so dramatic but also here the lateral current flow component is much more relevant than the vertical current flow. Since the distance of the rear contact points and the resulting contact coverage has an influence on the open-circuit voltage of PRC cells which is in contradiction to the trend in fill factor, the cell design and material choice will always be a trade-off between opposed requirements [6]. One cell structure which does not suffer from this dilemma is the classical screen-printed aluminium back surface field (Al-BSF) cell with its full-area back contact. Fig. 1 visualizes the difference in the majority current flow pattern at maximum power point (mpp) of a solar cell with full-area contact (BSF), partial rear contact (PRC), and interdigitated rear contact (IBC).

Based on the aforementioned facts, a desirable cell structure especially for a robust and cost-effective industrial production would be contacted on both sides and feature a full-area back contact with low carrier recombination. In order to enable a renaissance of this cell structure for upcoming PV generations, a new rear contact with much lower recombination current is needed to substitute the Al-BSF rear structure. Such structures are known as selective or passivated contacts [7] exhibiting excellent carrier selectivity. For a good overview about recent activities in this field see Ref. [8].

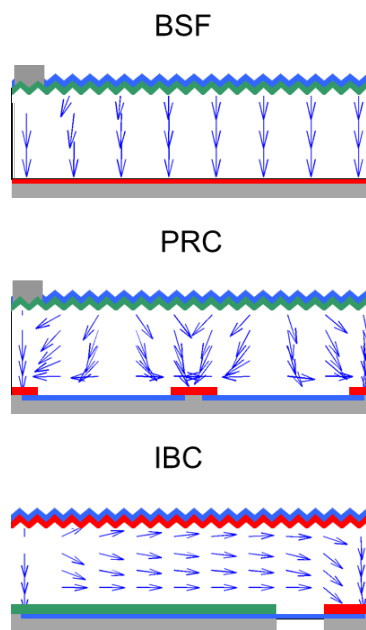


Fig. 1: Sketches of the majority current flow pattern at mpp of a full-area BSF, a PRC and an IBC solar cell (not to scale).

The most prominent example for a passivated contact is the heterojunction of amorphous and crystalline silicon commercialized under the trademark HIT by Sanyo/Panasonic [9]. This structure shows an extremely low recombination current resulting in very high open-circuit voltages up to 750 mV. Unfortunately, due to the use of amorphous silicon the structure does not withstand high-temperature budgets and has to be combined with a special metallization scheme. This paper will analyse the differences between PRC and full-area BSF cells and present an alternative approach for the fabrication of passivated contacts, the TOPCon approach [10].

## 2. ANALYSIS OF TRANSPORT LOSSES

To analyse the influence of different rear contact configurations, a Quokka [11] simulation of the cell structure shown in Fig. 2 was performed. As base material  $2 \Omega \text{ cm}$   $p$ -type silicon with a thickness of  $180 \mu\text{m}$  was chosen. We have assumed a high-quality emitter with a sheet resistance of  $150 \Omega/\text{sq}$  with excellent surface passivation. At the rear surface the cell is contacted with  $50 \mu\text{m}$  stripe-like contacts. The remaining surface is covered with a dielectric layer with excellent surface passivation quality ( $J_{0,\text{pass}} = 1 \text{ fA}/\text{cm}^2$ ). The distance between the rear contacts,  $d_{\text{cont}}$ , and their recombination current,  $J_{0,\text{cont}}$ , were varied over a wide range. Note that if  $d_{\text{cont}} = 0 \mu\text{m}$ , the cell has a full-area contact (contact area fraction = 100%). Assuming an ideal full-area rear contact ( $J_{0,\text{cont}} = 0 \text{ fA}/\text{cm}^2$ ) the investigated device would have a maximum open-circuit voltage of 730 mV.

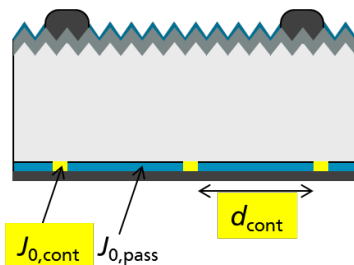


Fig. 2: Model for the simulation of the influence of contact distance or contact area fraction, respectively.

Fig. 3 shows the  $J_{0,\text{cont}}$  values which are necessary to achieve certain open-circuit voltages (700 mV, 710 mV, and 720 mV). When the contact distance,  $d_{\text{cont}}$ , is reduced,  $J_{0,\text{cont}}$  has to be reduced significantly to achieve the same open-circuit voltage. For a full-area contact it is not possible to achieve open-circuit voltages of 700 mV with typical values of full-area Al-BSFs (grey bar) even with the excellent emitter and bulk quality assumed in this study. Nevertheless, such open-circuit voltages are achievable with PRC structures with  $d_{\text{cont}}$  around  $500 \mu\text{m}$  due to reduced total contact recombination (which is of course the basic idea of the PRC concept). Thus, if a full-area contact is projected,  $J_{0,\text{cont}}$  values well below  $50 \text{ fA}/\text{cm}^2$  have to be achieved. Such low values cannot be realized with classical diffused or alloyed high-low junctions but passivated contact technologies are needed (see next section).

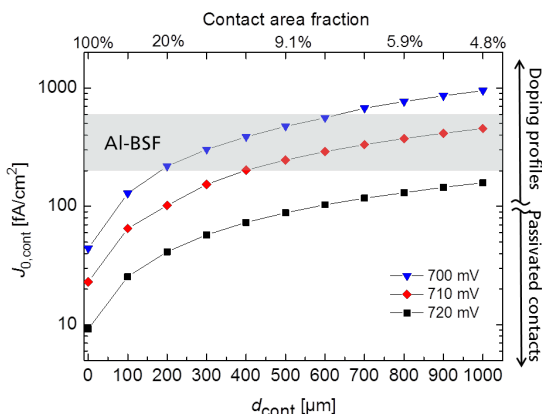


Fig. 3:  $J_{0,\text{cont}}$  values necessary to achieve certain open-circuit voltages for different rear contact distances.

Fig. 4 shows the efficiency potential of the same simulation. In principle the same trend as in Fig. 3 can be observed: Lower contact distances require lower  $J_{0,\text{cont}}$  values. However, it can also be observed that the efficiency potential for PRC cells with wider contact distances is limited. A closer look to situation at  $J_{0,\text{cont}} = 6 \text{ fA}/\text{cm}^2$  (see Fig. 5) shows that the FF is reduced for increasing contact distances due to the increasing lateral current component (see Fig. 1 b). This is a result of the aforementioned trade-off between recombination and transport optimization for PRC cells.

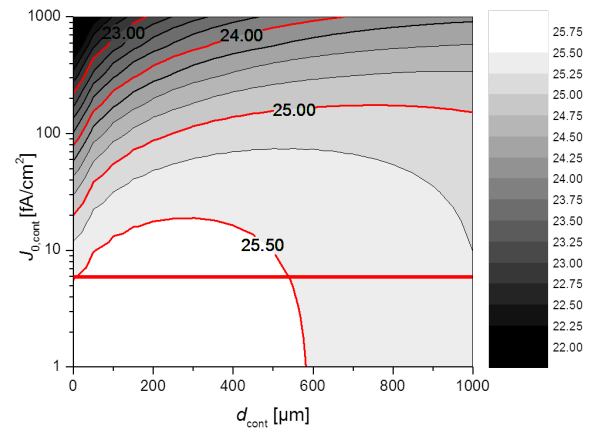


Fig. 4: Simulated efficiency potential of the cell structure shown in Fig. 2 as a function of  $J_{0,\text{cont}}$  and  $d_{\text{cont}}$ .

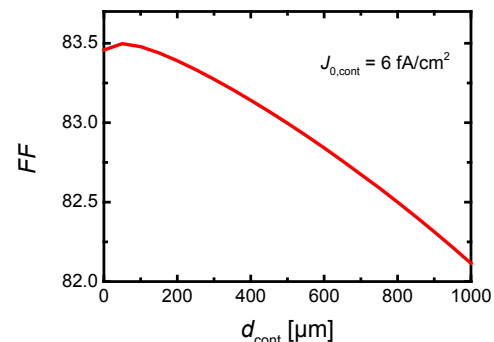


Fig. 5: FF for  $J_{0,\text{cont}} = 6 \text{ fA}/\text{cm}^2$  as a function of contact distance (red line in Fig. 4).

In an additional numerical simulation, we have also studied the influence of varying base resistivities for full-area BSF and PRC cells. It could be shown that full-area BSF cells have a much higher tolerance towards varying base resistivities than PRC cells. This study will be presented elsewhere [12].

It should be noted that the FF sensitivity of PRC cells presented in this chapter can be reduced if a total diffusion at the rear surface is introduced like in a PERT solar cell [4]. However, this would increase process complexity as compared to a PRC cell with Al-alloyed local contacts.

## 3. TOPCon TECHNOLOGY

In the TOPCon approach, developed at Fraunhofer ISE [10], the passivated contact is realized by the growth of an ultrathin tunnel oxide layer and the PECVD deposition of a thin highly doped silicon layer. The thickness of the oxide is rather critical as can be shown by simulations

[13]. If the oxide is too thin, the passivation quality will be reduced while thicker oxides hinder the majority carrier tunnel transport. In fact, the thickness of the tunnel oxide should be below 1.5 nm. Such oxides can be fabricated using wet-chemical [10] or UV/O<sub>3</sub> growth [14]. After the deposition of the silicon film, a high-temperature anneal and hydrogen passivation is performed to tune the morphology and the band gap of the silicon film. In this way we attempt to combine the advantages of a heterojunction a-Si/c-Si structure [15], i.e. excellent carrier selectivity (see Fig. 6 a) with the ones of a classical polysilicon-contact [16], i.e. higher temperature stability (see Fig. 6 b). For anneal temperatures between 700-900°C, a contact resistance of below 5 mΩ cm<sup>2</sup> and  $J_{0,cont}$  below 10 fA/cm<sup>2</sup> were achieved [17]. The lowest value achieved so far is 7 fA/cm<sup>2</sup> for an *n*-type contact.

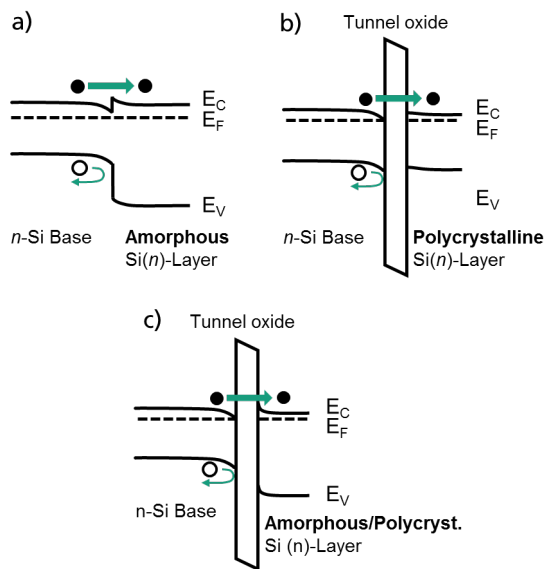


Fig. 6: Schematic concepts of different passivated contact technologies. a) a-Si/c-Si heterojunction, b) poly-Si with tunnel oxide, c) TOPCon.

Fig. 7 shows a colored TEM image of the TOPCon cross section. In this example, the tunnel oxide layer is around 1.2 nm to allow for an efficient charge carrier transport. It can be seen that the silicon film is a mixture of amorphous and crystalline phases. The ratio of amorphous and crystalline phases can be tuned by the final high-temperature anneal.

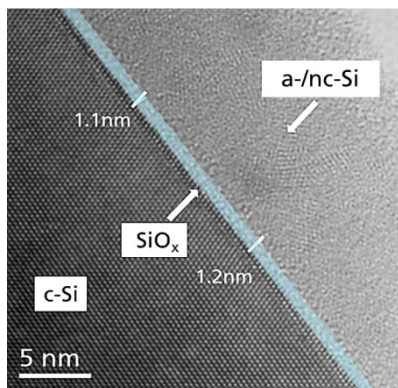


Fig. 7: TEM image of the cross section of the TOPCon structure.

#### 4. SOLAR CELL STRUCTURE

In our cell structure we aim to combine the advantages of a classical homojunction front side (Al<sub>2</sub>O<sub>3</sub>-passivated boron emitter), i.e. excellent optical transparency, and of a full-area passivated rear contact (TOPCon), i.e. excellent passivation. The full-area contact at the rear allows to keep the process complexity low and the current flow pattern simple. A schematic of the cell is shown in Fig. 7. As rear metal evaporated silver was chosen since it enables a high internal reflectivity [10]. The 2×2 cm<sup>2</sup> cells were fabricated on 200 μm thick 1 Ω cm FZ-Si *n*-type material. More details on the cell structure and process will be presented elsewhere.

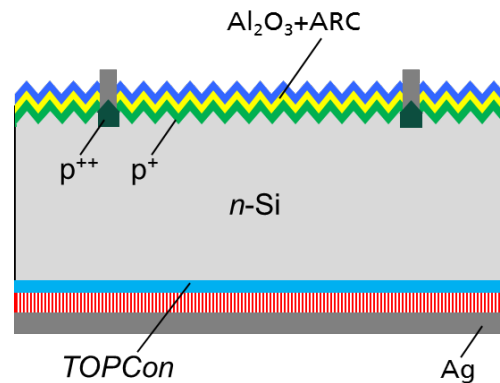


Fig. 8: Sketch of *n*-type solar cell with diffused front boron emitter and full-area rear passivated contact (TOPCon).

Note that although the cell structure is shown for the case of an *n*-type silicon base, the analogous architecture with a phosphorus-diffused emitter, a *p*-type silicon base and a *p*-TOPCon rear structure is also possible and currently under investigation.

We have performed Quokka and Sentaurus DEVICE [18] simulations of such a hybrid cells to study the influence of the base resistivity. The detailed Sentaurus study will be presented elsewhere [12]. Fig. 9 shows the Quokka simulation of the efficiency potential as function of base resistivity. While for base resistivities below 1 Ω cm the cell is limited by intrinsic Auger recombination in the bulk, our simulation shows that above this level the efficiency potential is independent of the base resistivity.

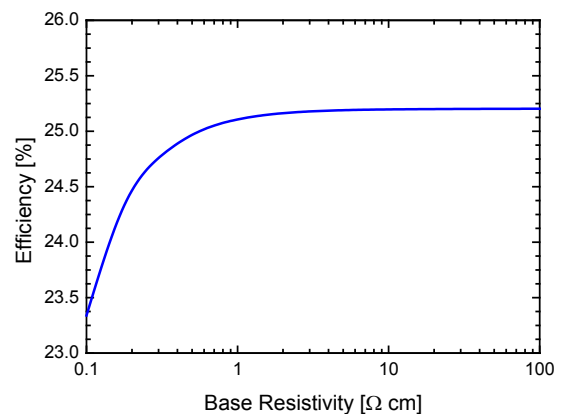


Fig. 9: Quokka simulation of the TOPCon cell structure (see Fig. 8) as a function of base resistivity.

## 5. RESULTS

Fig. 10 shows the measured normalized efficiency for different base resistivities. As was predicted in the simulation in the previous section (see Fig. 9), the efficiency potential of our TOPCon cell is rather independent of the chosen base resistivity. This is an advantage in production environment since a much wider doping range of the starting material can be accepted.

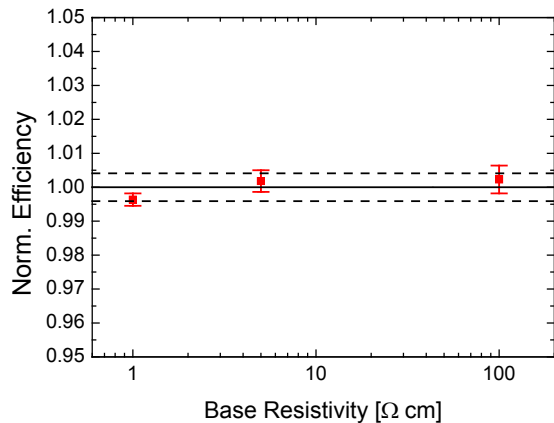


Fig. 10: Measured normalized efficiency of TOPCon cells (see Fig. 8) as a function of base resistivity.

Table I shows the IV-parameters of the best solar cell achieved so far (measured and confirmed by Fraunhofer ISE CalLab). The high open-circuit voltage shows that the excellent passivation of the surfaces of the silicon wafer can be maintained during all fabrication steps. Due to the excellent injection-dependent passivation quality, the pseudo fill factor ( $pFF$ ) of the final cells is above 85 %, which is a basic prerequisite [19] to achieve such high fill factors > 83 %.

**Table I:** IV-parameters of the recent  $n$ -type champion solar cell ( $2 \times 2$  cm<sup>2</sup>, designated area measurement). Cell results are confirmed at Fraunhofer ISE CalLab.

$V_{oc}$ [mV]	$J_{sc}$ [mA/cm <sup>2</sup> ]	$FF$ [%]	$\eta$ [%]
718	42.1	83.2	25.1

To get a more detailed view on the recombination statistics of the cell, Table II summarizes typical  $J_0$  contributions measured on test samples representing the different regions of the solar cell.

**Table III:** Summary of measured and calculated  $J_0$  values (area-weighted).

$J_{0,p+}$ [fA/cm <sup>2</sup> ]	$J_{0,c,cont}$ [fA/cm <sup>2</sup> ]	$J_{0,bulk}$ [fA/cm <sup>2</sup> ]	$J_{0,rear}$ [fA/cm <sup>2</sup> ]	$J_{0,total}$ [fA/cm <sup>2</sup> ]
13	2	8	7	~30

This analysis shows that around 50% of the recombination takes place at the front side of the cell. Therefore, the next step to further increase the efficiency of our cells is to improve the quality of the front emitter and contacts.

It should be noted that our TOPCon approach also works on multicrystalline silicon. A remarkable efficiency of 19.6% has been achieved on  $n$ -type multicrystalline silicon [20]. Additionally, the transfer to larger cell areas and industrial equipment is currently in progress at Fraunhofer ISE.

### Acknowledgement

The authors would like to thank the whole clean-room team at Fraunhofer ISE and all other colleagues which have contributed to this work. The TOPCon technology was developed within the project “ForTeS” (0325292) funded by the German Federal Ministry for Economic Affairs and Energy. We also acknowledge the fruitful cooperation with Georgia Tech and NREL supported by DOE within the FPACE II program.

### References

- [1] D. D. Smith, P. Cousins, S. Westerberg, R. De Jesus-Tabajonda, G. Aniero, and Y.-C. Shen, *Toward the practical limits of silicon solar cells*, IEEE Journal of Photovoltaics 6, pp. 1465-1469 (2014).
- [2] K. Masuko, M. Shigematsu, T. Hashiguchi, D. Fujishima, M. Kai, N. Yoshimura, T. Yamaguchi, Y. Ichihashi, T. Mishima, and N. Matsubara, *Achievement of more than 25% conversion efficiency with crystalline silicon heterojunction solar cell*, IEEE Journal of Photovoltaics 4, pp. 1433-1435 (2014).
- [3] J. Nakamura, N. Asano, T. Hieda, C. Okamoto, H. Katayama, and K. Nakamura, *Development of Heterojunction Back Contact Si Solar Cells*, IEEE Journal of Photovoltaics 4, pp. 1491-1495 (2014).
- [4] J. Zhao, A. Wang, and M. A. Green, *24.5% Efficiency silicon PERT cells on MCZ substrates and 24.7% efficiency PERL cells on FZ substrates*, Progress in Photovoltaics: Research and Applications 7, pp. 471-474 (1999).
- [5] M. A. Green, *The path to 25% silicon solar cell efficiency: History of silicon cell evolution*, Progress in Photovoltaics 17, pp. 183-189 (2009).
- [6] K. R. Catchpole and A. W. Blakers, *Modelling the PERC structure for industrial quality silicon*, Solar Energy Materials and Solar Cells 73, pp. 189-202 (2002).
- [7] U. Würfel, A. Cuevas, and P. Würfel, *Charge carrier separation in solar cells*, IEEE Journal of Photovoltaics 5, pp. 461-469 (2015).
- [8] A. Cuevas, T. Allen, J. Bullock, Y. Wan, D. Yan, and X. Zhang, *Skin care for healthy silicon solar cells*, IEEE Photovoltaic Specialists Conference New Orleans (2015)
- [9] M. Taguchi, A. Yano, S. Tohoda, K. Matsuyama, Y. Nakamura, T. Nishiwaki, K. Fujita, and E. Maruyama, *24.7% record efficiency HIT solar cell on thin silicon wafer*, IEEE Journal of Photovoltaics 4, pp. 96-99 (2014).
- [10] F. Feldmann, M. Bivour, C. Reichel, M. Hermle, and S. W. Glunz, *Passivated rear contacts for high-efficiency  $n$ -type Si solar cells providing high interface passivation quality and excellent transport characteristics*, Solar Energy Materials and Solar Cells 120, pp. 270-274 (2014).
- [11] A. Fell, *A free and fast three-dimensional/two-dimensional solar cell simulator featuring conductive boundary and quasi-neutrality approximations*, IEEE Transactions on Electron Devices 60, pp. 733-738 (2013).
- [12] H. Steinkemper et al., to be published (2015).

- [13] H. Steinkemper, F. Feldmann, M. Bivour, and M. Hermle, *Numerical simulation of carrier-selective electron contacts featuring tunnel oxides*, IEEE Journal of Photovoltaics 5, pp. 1348-1356 (2015).
- [14] A. Moldovan, F. Feldmann, M. Zimmer, J. Rentsch, J. Benick, and M. Hermle, *Tunnel oxide passivated carrier-selective contacts based on ultra-thin SiO<sub>2</sub> layers*, Solar Energy Materials and Solar Cells 142, pp. 123-127 (2015).
- [15] M. Taguchi, K. Kawamoto, S. Tsuge, T. Baba, H. Sakata, M. Morizane, K. Uchihashi, N. Nakamura, S. Kiyama, and O. Oota, *HIT<sup>TM</sup> cells - high-efficiency crystalline Si cells with novel structure*, Progress in Photovoltaics: Research and Applications 8, pp. 503-513 (2000).
- [16] I. R. C. Post, P. Ashburn, and G. R. Wolstenholme, *Polysilicon emitters for bipolar transistors: a review and re-evaluation of theory and experiment*, IEEE Transactions on Electron Devices 39, pp. 1717-1731 (1992).
- [17] F. Feldmann, *Advanced passivated contacts and their applications to high-efficiency cells*, Workshop on Crystalline Silicon Solar Cells and Modules, Keystone, CO (2015)
- [18] Synopsis, *Synopsis TCAD*, Rel. H-2013.03 [Online]. Available: <http://www.synopsys.com> (2013).
- [19] M. Bivour, *Device physics of hetero-junction solar cells*, Workshop on Crystalline Silicon Solar Cells and Modules, Breckenridge, CO (2014)
- [20] F. Schindler, J. Schön, B. Michl, P. Krenckel, S. Riepe, F. Feldmann, J. Benick, M. Hermle, S. W. Glunz, W. Warta, and M. C. Schubert, *High-efficiency multicrystalline silicon solar cells: Potential of n-type Doping*, IEEE Journal of Photovoltaics (2015).